Contribution from the Department of Chemistry,
University of Texas, Austin, Texas 78712

Amino Acid Substituted Iron Porphyrins. 2. Thermodynamic Studies of Ligand Binding

H. GOFF and L. O. MORGAN*

Received October 21, 1975 AIC507615

Equilibrium quotients have been obtained for axial ligand binding to iron(II) and iron(III) 2,4-dicysteine-substituted mesoporphyrin (heme *c* and hemin *c*, respectively) in aqueous solution near neutral pH. Variation in ionic strength, pH, and buffer resulted in relatively small changes in equilibrium quotients, but the values were affected by significant iron porphyrin dimerization. Cyanide ion binding was found to occur in a stepwise manner, whereas only the overall equilibrium for two-ligand binding was observed for the other ligands studied. Enthalpy and entropy changes were determined indirectly from temperature dependence of equilibrium quotients. For a given ligand, enthalpy changes are more favorable for binding to the iron(II) porphyrin than to the iron(III) porphyrin, but entropy changes are of the opposite order. In terms of favorable enthalpy changes, the ligand binding orders were found to be cyanide ion > L-histidine > imidazole > pyridine for hemin *c* and cyanide ion > pyridine > L-histidine > imidazole > *N*-acetyl-DL-methionine for heme *c*. Enthalpy and entropy changes were also determined for cyanide ion displacement of a single dipeptide histidine ligand in the iron(II) and iron(III) 2,4-bis(cysteinylhistidine) dipeptide substituted mesoporphyrin (heme(Cys-His)$_2$ and hem(Cys-His)$_2$, respectively).

Introduction

Iron porphyrins have long been employed in attempts to understand details of ligand binding in the parent hemoprotein molecules. However, common iron porphyrins (e.g., iron protoporphyrin IX) exhibit low water solubility at neutral pH and dimerize even at very low concentrations unless mixed solvents or detergent solutions are used. Equilibrium quotients reported by early workers for ligand binding to these aggregated iron porphyrins are generally of only qualitative significance, since the equilibria were inadequately defined.[1-4] Ligand binding work has been done in aqueous detergent solutions, but equilibrium quotients are dependent on the concentration and nature of the detergent.[5,6] More recently, to avoid solubility and aggregation problems and to simulate the generally hydrophobic environment in the protein, ligand-binding studies have been done in nonaqueous media.[7-14] Although the equilibria are expected to be more straightforward, large disparities in equilibrium quotients have been noted among different workers.[7,12]

Since the porphyrin is at least partially exposed to solvent in many hemoproteins, water remains a desirable medium for iron porphyrin ligand-binding studies. Adequate solubility of a variety of ligands also adds to the attractiveness of aqueous media. The relevance, but paucity, of quantitative ligand-binding data in aqueous solution directed us to an extensive study of ligand binding to amino acid substituted iron porphyrins containing the prosthetic group of cytochrome *c*. Aqueous solution properties and dimerization tendencies of the 2,4-dicysteine-substituted iron mesoporphyrin (heme *c* and hemin *c*[15]) and the 2,4-biscysteinylhistidine dipeptide substituted iron mesoporphyrin (heme(Cys-His)$_2$ and hem-(Cys-His)$_2$[15]) have been studied previously.[16] Since equilibrium quotients are unreliable for comparison of ligand-binding strengths, unless the entropy term is constant, enthalpy and entropy data have been obtained indirectly by measuring temperature dependence of the equilibrium quotients for both the iron(II) and iron(III) porphyrins.

Experimental Section

Iron(III) porphyrins were prepared, purified, and analyzed as previously described.[16] Imidazole was purified by fivefold recrystallization from benzene followed by vacuum-drying. Pyridine was distilled after drying over solid potassium hydroxide. Other commercially available ligands were used directly. Imidazole, pyridine, amino acids, and amino acid derivatives were standardized by potentiometric titration and sodium cyanide was standardized by silver nitrate titration.[17] Stock ligand solutions were prepared fresh daily. Stock hemin solutions were protected from light and used not more than 4 h after preparation. Spectral measurements were made on ligand-containing hemin solutions within a few minutes of preparation and on heme solutions within a few minutes of reduction, except for heme *c* solutions containing relatively large amounts of cyanide ion, which showed kinetically complex spectral changes requiring 20–30 min for completion after sodium dithionite addition.

Air-sensitive iron(II) porphyrins were prepared in solution from the corresponding iron(III) porphyrins by reduction with a small excess of solid sodium dithionite in a specially designed anaerobic cell. Hemin–ligand solutions were degassed by freeze–pump–thaw cycles, the hemin solution was treated with sodium dithionite, and spectrophotometric measurements were made with the solution under high vacuum. Carbon monoxide was added to the anaerobic cell at 100–200 Torr to produce carbonylated iron(II) complexes.

An Orion Model 701 pH meter calibrated with NBS tolerance buffers was used for pH measurements at the temperature of the spectrophotometric study. Spectrophotometric measurements were made with Cary 14 and Beckman DU instruments. The Beckman DU was equipped with a thermostated cell compartment controlled to ±0.1 °C. Magnetic measurements were made as previously described by the NMR technique (Evans' method).[16,18]

Results and Treatment of Data

Binding of axial ligands to iron porphyrins may be described by (charges and axial solvent ligands not shown)

$$\mathrm{Fe(por)} + \mathrm{L} \overset{Q_1}{\rightleftharpoons} \mathrm{Fe(por)L} \tag{1}$$

$$\mathrm{Fe(por)L} + \mathrm{L} \overset{Q_2}{\rightleftharpoons} \mathrm{Fe(por)L_2} \tag{2}$$

$$\mathrm{Fe(por)} + 2\mathrm{L} \overset{Q_{12}}{\rightleftharpoons} \mathrm{Fe(por)L_2} \tag{3}$$

Provided only one of these equilibria is operative in a study of ligand addition to iron porphyrin solutions, the equilibrium quotient Q_i (Q_1, Q_2, or Q_{12}) may be obtained from spectrophotometric measurements by

$$Q_i = \frac{[\mathrm{Fe(por)L}_{p+n}]}{[\mathrm{Fe(por)L}_p][\mathrm{L}]^n} = \frac{\epsilon - \epsilon_0}{\epsilon_\infty - \epsilon}\,\frac{1}{[\mathrm{L}]^n} \tag{4}$$

where ϵ is the molar absorptivity for partially ligated solutions, ϵ_0 is for iron porphyrin solutions alone, ϵ_∞ is for completely ligated iron porphyrin solutions, and p is 0 or 1. The value of n may be obtained from the slope of a log plot of eq 4

$$\log \frac{\epsilon - \epsilon_0}{\epsilon_\infty - \epsilon} = n \log [\mathrm{L}] + \log Q_i \tag{5}$$

If ϵ_∞ cannot be obtained directly, eq 4 may be rearranged to a linear equation[19]

$$\epsilon = \epsilon_\infty - \frac{1}{Q_i}\,\frac{\epsilon - \epsilon_0}{[\mathrm{L}]^n} \tag{6}$$

from which plots of ϵ vs. $(\epsilon - \epsilon_0)/[\mathrm{L}]^n$ yield $-1/Q_i$ as slope and ϵ_∞ as intercept.

Considerable debate has raged concerning use of the Benesi–Hildebrand analysis to arrive at expressions such as eq 5 and eq 6.[20] Rose and Drago[20a] have devised a general

Table I. Absorption Spectra of Iron Porphyrin Complexes[a]

	Wavelength max, nm ($10^{-3}\epsilon$, M^{-1} cm^{-1})
Iron(III) Porphyrins[b]	
Hemin *c*[c]	393 (168), 493 (7.26), 615 (3.36)
Dihistidylhemin *c*	405 (118), 527 (9.67)
Bis(imidazole)hemin *c*	405 (121), 527 (9.67)
Bis(pyridyl)hemin *c*	400 (115), 525 (10.1)
Cyanohemin *c*	406 (118), 530 (9.70)
Dicyanohemin *c*	418 (95.9), 541 (10.7)
Hem(Cys-His)$_2$	406 (120), 528 (9.20)
Hem(Cys-His)$_2$(CN)[d]	411 (110), 533 (9.71)
Iron(II) Porphyrins[d]	
Heme *c*[c]	412.5 (122), 542 (9.32), 560 (8.33)
Dihistidylheme *c*	414 (159), 520 (12.2), 549 (20.0)
Bis(imidazole)heme *c*	414 (159), 520 (13.2), 549 (21.4)
Bis(pyridyl)heme *c*	408 (133), 517 (14.4), 547 (26.3)
Bis(*N*-acetylmethionyl)heme *c*	424 (96.0), 523 (13.2), 552 (14.8)
Cyanoheme *c*	409 (124), 518 (14.7), 547 (24.0)
Dicyanoheme *c*	428 (119), 532 (17.1), 561 (10.2)
Carbonylheme *c*	403 (220), 526 (11.8), 558 (13.5)
heme(Cys-His)$_2$	415.5 (160), 521 (13.4), 550 (21.5)
heme(Cys-His)$_2$(CN)	419 (121), 525 (14.8), 553 (16.9)
heme(Cys-His)$_2$(CO)	411.5 (191), 531 (11.7), 560 (9.00)

[a] $I = 0.10$ with $NaClO_4$; 0.01 M phosphate buffer; 25 °C; uncertainties in ϵ values are approximately ±2%. [b] pH 6.0. [c] $I = 0.01$; molar absorptivity coefficients are extrapolated to zero porphyrin concentration. [d] pH 7.0.

method whereby a graphical or numerical analysis is obtained by trial choices of ϵ_∞, the molar absorptivity of the complex. A set of absorbance values is obtained from solutions containing varying amounts of ligand, and a curve is drawn for each absorbance measurement. If the system is properly defined, the curve intersections should cluster in a small area from which the equilibrium quotient (equilibrium constant if activities are known) and true ϵ_∞ values are obtained.

L-Histidine, Imidazole, and Pyridine Binding to Hemin *c*. Addition of L-histidine, imidazole, or pyridine to hemin *c* solutions shifts the near-ultraviolet Soret band to longer wavelengths and produces changes in the visible region absorption bands (see Table I). Concentration and pH conditions were chosen so that an insignificant amount of hemin *c* was in the dimeric form (~3%).[16] Ligand concentration was varied in individual experiments to produce typically 12–87% ligated hemin *c*. Values of *n* not significantly different from 2.0 were obtained from application of eq 5, and only values of $n = 2.0$ yielded linear plots of eq 6. Isosbestic points were observed, the equilibrium quotient was independent of wavelength, and Coleman–Varga–Mastin (CVM) plots[21] were consistent with the presence of only two absorbing species. Use of eq 6 or graphical analysis by the method of Rose and Drago[20a] yielded equivalent values. No spectral evidence was found for addition of a single L-histidine, imidazole, or pyridine ligand to hemin *c*. Equilibrium quotients were calculated on the basis of unprotonated ligand concentration from available thermodynamic acid dissociation data at or near ionic strength 0.10 for L-histidine ($\Delta H = 8.73$ kcal/mol, $\Delta S = 1.52$ eu),[22] imidazole ($\Delta H = 8.395$ kcal/mol, $\Delta S = -3.87$ eu),[23] pyridine ($\Delta H = 4.795$ kcal/mol, $\Delta S = -7.55$ eu),[24] and *N*-acetyl-L-histidine ($pK_a(25\ °C) = 7.08$).[25] Since ligand concentration was much greater than hemin *c* concentration, ligand concentration at equilibrium was assumed equal to the amount added. Equilibrium quotients obtained by eq 6 for L-histidine, imidazole, and pyridine binding to hemin *c* are listed in Table II.

Table II. Equilibrium Quotients for L-Histidine, Imidazole, and Pyridine Binding to Hemin *c*[a]

Temp, °C	pH	Q_{12}, M^{-2}	Temp, °C	pH	Q_{12}, M^{-2}
		L-Histidine			
15.5	6.27	8.82×10^4 [b]	25.0	7.08	2.44×10^4 [c]
20.5	6.18	6.26×10^4 [b]	25.0	6.00	5.05×10^4 [b,d]
25.0	6.10	4.60×10^4 [b]	25.0	5.98	4.51×10^4 [b,e]
29.0	6.05	3.50×10^4 [b]	23.5	6.54	4.79×10^4 [f]
33.0	5.98	2.66×10^4 [b]	25.0	6.12	3.57×10^4 [g]
37.0	5.94	2.06×10^4 [b]	25.0	6.08	4.76×10^4 [b,h]
25.0	5.50	6.18×10^4 [b]	25.0	5.97	4.74×10^4 [b,i]
25.0	6.55	4.72×10^4 [c]	25.0	6.51	48.5×10^4 [c,j]
		Imidazole			
15.5	6.12	16.3×10^5 [b]	33.0	5.92	6.16×10^5 [b]
20.5	6.07	12.2×10^5 [b]	37.0	5.88	4.26×10^5 [b]
25.0	6.03	10.5×10^5 [b]	25.0	5.54	13.8×10^5 [b]
29.0	5.98	7.69×10^5 [b]	25.0	6.46	11.2×10^5 [c]
		Pyridine			
15.5	6.15	16.3×10^2 [b]	29.0	6.00	10.3×10^2 [b]
20.5	6.09	14.3×10^2 [b]	33.0	5.97	7.47×10^2 [b]
25.0	6.03	12.4×10^2 [b]	37.0	5.90	6.41×10^2 [b]

[a] $I = 0.10$ with $NaClO_4$; 0.01 M phosphate buffer; Q values are ±4% at one standard deviation. [b] 5×10^{-6} M hemin *c*. [c] 3×10^{-6} M hemin *c*. [d] $I = 0.025$. [e] $I = 0.30$. [f] 1.3×10^{-6} M hemin *c*. [g] 2.8×10^{-5} M hemin *c*. [h] 1×10^{-3} M phosphate buffer. [i] 0.01 M Pipes buffer. [j] *N*-Acetyl-L-histidine.

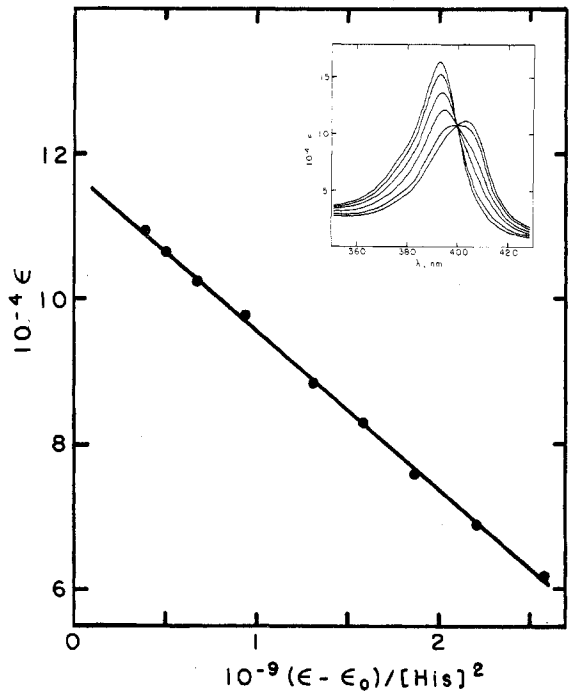

Figure 1. Hemin *c* titration with L-histidine, for 5×10^{-6} M hemin *c*, pH 6.1, $I = 0.10$, 0.01 M phosphate buffer, 25 °C, and ϵ values at 405 nm.

Typical plots of L-histidine binding to hemin *c* are shown below. Figure 1 contains spectra of a hemin *c* titration with L-histidine and a linear curve corresponding to analysis by eq 6. Values of $Q_{12} = 4.60 \times 10^4$ M^{-2} and $\epsilon_\infty = 1.18 \times 10^5$ M^{-1} cm^{-1} were obtained. Figure 2 shows a typical CVM plot[21] for two absorbing species in the hemin *c*–histidine system. The linear curves and convergence at the zero intercept confirm

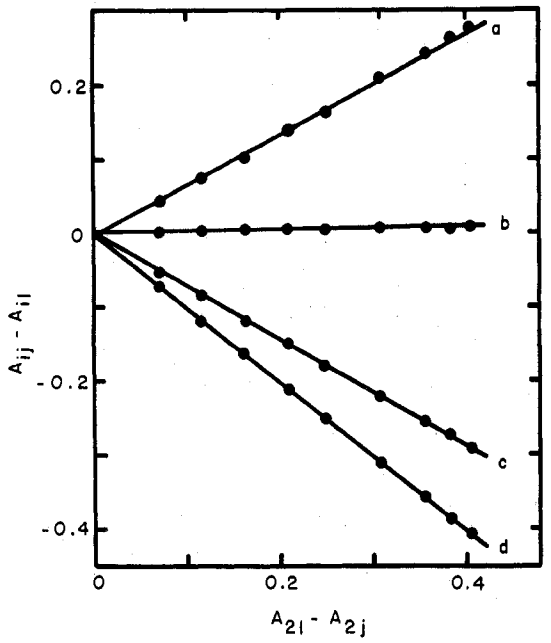

Figure 2. CVM plot for two absorbing species, hemin *c* and L-histidine, at 5×10^{-6} M hemin *c*, pH 6.1, $I = 0.10$, 0.01 M phosphate buffer, and 25 °C: (a) 405 nm; (b) 400 nm; (c) 385 nm; (d) 393 nm.

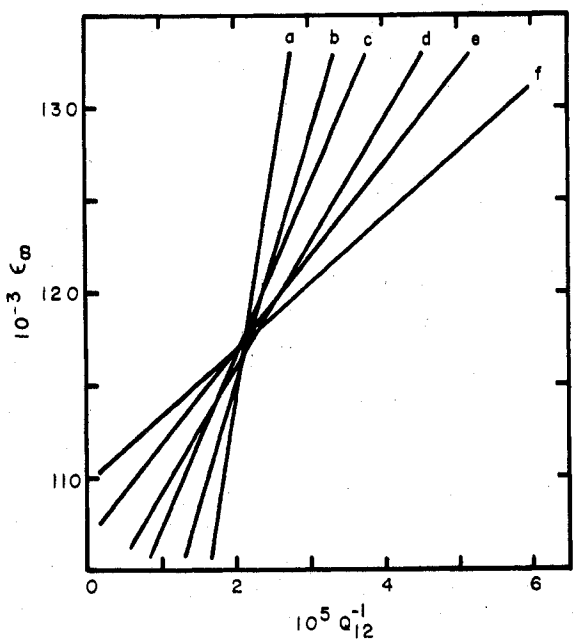

Figure 3. Rose-Drago plot for hemin *c* + L-histidine, at 5×10^{-6} M hemin *c*, pH 6.1, $I = 0.10$, 0.01 M phosphate buffer, 25 °C, 405 nm, and total histidine concentrations of (a) 1.694×10^{-3} M, (b) 5.08×10^{-3} M, (c) 6.78×10^{-3} M, (d) 8.47×10^{-3} M, (e) 1.016×10^{-2} M, and (f) 1.186×10^{-2} M.

the existence of only two absorbing species. A typical Rose–Drago plot is shown in Figure 3 for the same data contained in Figure 1. A near-common intersection of all of the curves indicates that the system is well defined.[20] Values of $Q_{12} = 4.65 \times 10^4$ M^{-2} and $\epsilon_\infty = 117.5$ M^{-1} cm^{-1} were obtained. That results from the Rose–Drago treatment are identical with those from eq 6 is not surprising, since under the conditions employed here where [ligand] ≫ [iron porphyrin] the Rose–Drago treatment reduces to eq 6 (also known as the Ketelaar equation[20a]).

L-Histidine, Imidazole, Pyridine, and *N*-Acetyl-DL-methionine Binding to Heme *c*. Because of small spectral changes in the Soret absorption band of heme *c* (see Table I), precise ligand-binding data for the ligands listed above could only be obtained by observing spectral changes in the visible region, and lower intensity of the visible absorption bands necessitated using heme *c* concentrations at which a significant amount of heme *c* was present in dimeric form (22% for a 2×10^{-5} M unligated heme *c* solution).[16] Assuming that ligand coordination occurs only with monomeric heme *c*, the dimerization equilibrium

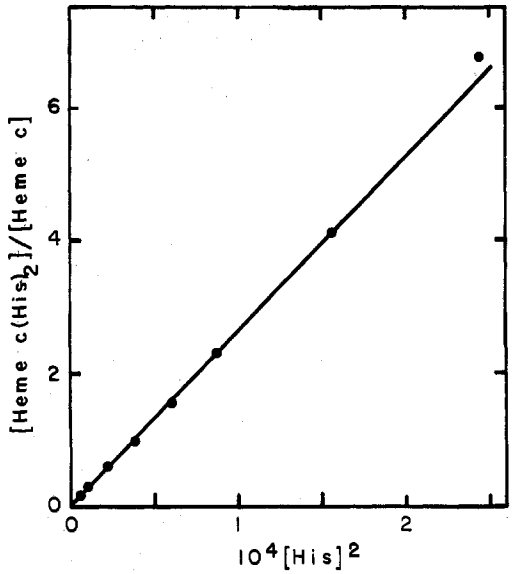

Figure 4. Heme *c* titration with L-histidine, for 2×10^{-5} M heme *c*, pH 7.0, $I = 0.10$, 0.01 M phosphate buffer, 25 °C, and ϵ values at 549 nm.

$$2\text{Fe(por)} \overset{Q_D}{\rightleftharpoons} [\text{Fe(por)}]_2 \tag{7}$$

is expected to compete with ligand binding. For ligand binding as expressed in eq 1 or eq 3 and by using the approximation that in the visible region spectra of the monomer and dimer are equivalent, the following expression may be derived

$$Q_i = \frac{[\text{Fe(por)L}_{p+n}]}{[\text{Fe(por)L}_p][\text{L}]^n} = \frac{4Q_D(A - A_0)}{(\epsilon_\infty - \epsilon_0)\left[-1 + \left(1 + \frac{8Q_D(A_\infty - A)}{(\epsilon_\infty - \epsilon_0)}\right)^{1/2}\right][\text{L}]^n} \tag{8}$$

where Q_D is the dimerization equilibrium quotient for heme *c*, and A_0, A, and A_∞ refer to absorbance values for unligated, partially ligated, and completely ligated heme *c* solutions. Considering the large spectral differences between ligated and unligated heme *c* and the predominance of monomeric material, assumption of equivalence of monomer and dimer spectra (differing by ~15% in the 550-nm region) appears to be a useful device to simplify an otherwise complex relationship for which the dimer molar absorptivity must be accurately known. A Q_D value of 1×10^4 M^{-1} was used for all calculations, since no measurable differences were obtained in the dimerization constant at pH values near neutrality at 15, 25, and 35 °C. A plot of $[\text{Fe(por)His}_2]/[\text{Fe(por)}]$ vs. $[\text{histidine}]^2$ as evaluated by eq 8 for a series of solutions with constant iron porphyrin concentration and variable amounts of ligand is shown in Figure 4. The intercept of such plots was generally within one standard deviation of zero. Equilibrium quotients for L-histidine, imidazole, pyridine, and *N*-acetyl-DL-methionine were obtained from the slope of such plots representing typically a range of 12–87% ligated material.

Table III. Equilibrium Quotients for L-Histidine, Imidazole, *N*-Acetyl-DL-methionine, and Pyridine Binding to Heme *c*[a]

Temp, °C	pH	Q_{12}, M^{-2}	Temp, °C	pH	Q_{12}, M^{-2}
		L-Histidine			
15.5	7.05	6.00×10^4 [b]	36.5	7.01	0.95×10^4 [b]
20.5	7.04	3.90×10^4 [b]	25.0	6.52	2.09×10^4 [b]
25.0	7.01	2.62×10^4 [b]	25.0	8.00	3.14×10^4 [b]
30.5	7.04	1.42×10^4 [b]	25.0	6.97	1.69×10^4 [b,e]
		Imidazole			
15.5	7.11	28.3×10^4 [b]	36.5	6.96	4.70×10^4 [b]
20.5	7.08	16.7×10^4 [b]	25.0	6.98	12.3×10^4 [b,g]
25.0	7.00	11.6×10^4 [b]	25.0	6.94	12.5×10^4 [b,h]
30.5	6.98	7.34×10^4 [b]			
		N-Acetyl-DL-methionine			
15.5	7.01	13.9×10^2 [c]	36.5	6.98	3.40×10^2 [c]
20.5	6.99	10.7×10^2 [c]	25.0	6.97	8.20×10^2 [d]
25.0	6.96	8.44×10^2 [c]	25.0	7.95	7.76×10^2 [c]
30.5	6.99	4.43×10^2 [c]	25.0	7.00	1.92×10^2 [c,f]
		Pyridine			
15.5	7.04	12.9×10^5 [b]	30.5	6.95	2.47×10^5 [b]
20.5	7.00	7.38×10^5 [b]	36.5	6.94	1.42×10^5 [b]
25.0	6.94	4.11×10^5 [b]			

[a] $I = 0.10$ with $NaClO_4$; 0.01 M phosphate buffer; Q values are ±4% at one standard deviation. [b] 2×10^{-5} M heme *c*. [c] 3×10^{-5} M heme *c*. [d] 5×10^{-6} M heme *c*. [e] *N*-Acetyl-L-histidine. [f] DL-Methionine. [g] 5×10^{-4} M phosphate buffer. [h] 0.01 M Pipes buffer.

Linear relationships could only be obtained for these ligands by using $n = 2.0$, and no spectral evidence was found for a monoligand adduct. A weighted linear least-squares scheme was employed, with weights proportional to the inverse square of the dependent variable.[26] Concentrations of unprotonated ligand were used in the calculations and the approximation was made that the equilibrium ligand concentration was equal to the added ligand concentration. Table III lists Q_{12} values for ligand binding to heme *c*.

Cyanide Ion Binding to Heme *c*. Addition of sodium cyanide to heme *c* solutions shifts the Soret absorption band to shorter wavelengths at relatively low cyanide ion concentrations, but high cyanide ion concentrations shift the band to longer wavelengths. Corresponding changes are observed at the visible absorption bands (see Table I). This behavior was shown to be consistent with stepwise cyanide ion binding as described by eq 1 and 2. Although the two equilibria overlapped somewhat, it was possible to observe typically 10–70% of the first equilibrium and 35–90% of the second equilibrium with no significant amounts (~2%) of dicyanoheme *c* and heme *c* present respectively. Values of Q_1 were evaluated by use of eq 8 where $n = 1.0$. Concentrations of free cyanide ion were calculated from thermodynamic parameters for acid dissociation ($\Delta H = 10.4$ kcal/mol, $\Delta S = -7.4$ eu).[27]

Cyanide ion binding to cyanoheme *c* (i.e., the Q_2 value) was found to be essentially independent of heme *c* concentration, and acceptable fits were obtained for eq 6 with $n = 1.0$, implying the monomeric nature of cyanoheme *c*. The straightforward equilibrium expressed by eq 2 is substantiated by the presence of isosbestic points, CVM plots for two absorbing species, independence of Q_2 on wavelength, and equivalent Q_2 values obtained by the method of Rose and Drago. Equilibrium quotients for cyanide ion binding to heme *c* are listed in Table IV.

Cyanide Ion Binding to Hemin *c*. Spectra of hemin *c* solutions containing cyanide ion, shown in the insert to Figure 5, reveal different isosbestic points at low and high cyanide ion concentrations. As was the case for heme *c* cyanide ion binding, this observation may be rationalized by stepwise equilibria described by eq 1 and 2. However, hemin *c*

Table IV. Equilibrium Quotients for Cyanide Ion Binding to Heme *c*[a]

Temp, °C	pH	$10^{-5}Q_1$, M^{-1}	pH	$10^{-3}Q_2$, M^{-1}
16.0	6.53	10.1[b]	7.03	13.5[c]
20.5	6.52	5.86[b]	7.02	9.15[c]
25.0	6.50	4.72[b]	7.00	8.16[c]
30.5	6.49	2.93[b]	6.99	6.71[c]
36.0	6.47	2.02[b]	6.97	4.69[c]
25.0	6.00	4.52[b]	6.52	8.55[c,d]
25.0	7.00	4.98[b]	8.03	7.02[c]
25.0	6.50	4.25[e]	7.00	8.51[b]

[a] $I = 0.10$ with $NaClO_4$; 0.01 M phosphate buffer; Q values are ±4% at one standard deviation. [b] 3×10^{-5} M heme *c*. [c] 5×10^{-6} M heme *c*. [d] $I = 0.30$. [e] 6×10^{-5} M heme *c*.

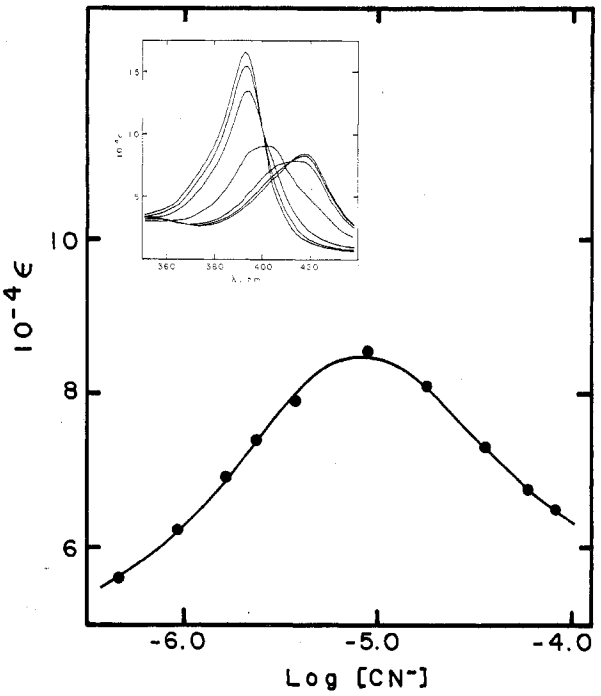

Figure 5. Hemin *c* titration with cyanide ion, for 5×10^{-6} M hemin *c*, pH 6.0, $I = 0.10$, 0.01 M phosphate buffer, 25 °C, and ϵ values at 406 nm; curve represents fit to eq 9.

equilibria were found to overlap to such an extent that precise analysis by eq 6 was not possible. Such overlapping equilibria may be evaluated from the relationship[28]

$$\epsilon = \frac{\epsilon_0 + \epsilon_1 Q_1 [L] + \epsilon_2 Q_1 Q_2 [L]^2}{1 + Q_1 [L] + Q_1 Q_2 [L]^2} \quad (9)$$

where ϵ and ϵ_0 are molar absorptivities for partially ligated and unligated hemin *c*, whereas ϵ_1 and ϵ_2 are for cyanohemin *c* and dicyanohemin *c*. Using values of ϵ_1 and ϵ_2 determined by Ang's method,[29] Q_1 and Q_2 were obtained by nonlinear least-squares analysis of eq 9.[30] Equilibrium quotients determined in this way were equivalent to values obtained by Ang's method and to estimates obtained at relatively low and high cyanide ion concentrations using eq 6. A plot of ϵ at 406 nm vs. log [CN^-] is shown in Figure 5 (a log scale is used due to the wide range of cyanide ion concentrations) with the curve representing the nonlinear least-squares result. Equilibrium quotients are listed in Table V.

Ligand Binding to hem(Cys-His)$_2$ and heme(Cys-His)$_2$. Addition of cyanide ion to hem(Cys-His)$_2$ and heme(Cys-His)$_2$ resulted in the small, but significant spectral changes shown in Table I. Analysis of spectral changes using eq 6 where $n = 1.0$ yielded linear plots and the equilibrium quotients listed in Table VI. Isosbestic points, CVM plots for two absorbing

Table V. Equilibrium Quotients for Cyanide Ion Binding to Hemin c[a]

Temp, °C	pH	$10^{-5}Q_1$, M^{-1}	$10^{-4}Q_2$, M^{-1}
17.0	6.03	3.37[b]	9.78[b]
21.0	6.02	3.12[b]	7.23[b]
25.0	6.00	2.64[b]	6.50[b]
29.0	5.99	2.13[b]	5.41[b]
33.0	5.98	1.88[b]	4.68[b]
37.0	5.97	1.47[b]	3.93[b]
25.0	5.50	3.27[b]	9.42[b]
25.0	6.50	2.53[b]	7.27[b]
25.0	6.00	2.95[c]	6.78[c]
22.5	6.00	2.25[d]	6.28[d]

[a] $I = 0.10$ with $NaClO_4$; 0.01 M phosphate buffer; Q values are ±4% at one standard deviation. [b] 5×10^{-6} M hemin c. [c] 1×10^{-5} M hemin c. [d] 1×10^{-6} M hemin c.

Table VI. Equilibrium Quotients for Cyanide Ion Binding to hem(Cys-His)$_2$ and heme(Cys-His)$_2$[a]

hem(Cys-His)$_2$			heme(Cys-His)$_2$		
Temp, °C	pH	$10^{-3}Q_1$,[b,c] M^{-1}	Temp, °C	pH	$10^{-4}Q_1$,[d,e] M^{-1}
16.0	7.03	11.9	15.5	7.02	22.1
20.5	7.02	10.9	20.5	7.00	14.4
25.0	7.00	7.94	25.0	6.96	7.66
30.5	6.99	6.27	30.5	6.97	4.21
36.0	6.97	4.74	36.5	6.96	2.39
25.0	6.52	10.4			
25.0	7.50	4.78			
25.0	8.00	4.02			

[a] $I = 0.10$ with $NaClO_4$; 0.01 M phosphate buffer. [b] Q values are ±4% at one standard deviation. [c] 5×10^{-6} M hem(Cys-His)$_2$. [d] Q values are ±7% at one standard deviation. [e] 2×10^{-5} M heme(Cys-His)$_2$.

species, Q_1 independence of wavelength, and equivalent Q_1 values obtained by the method of Rose and Drago suggest that one cyanide ion binds by displacement of a histidine ligand. The reversibility of this process has been demonstrated by dilution experiments and pH adjustment. Assuming displacement of the second histidine ligand by cyanide ion would produce spectra identical with those of dicyanohemin c and dicyanoheme c, an upper limit on Q_2 for hem(Cys-His)$_2$ and heme(Cys-His)$_2$ is 25 M^{-1}.

Addition of L-histidine, imidazole, or N-acetyl-DL-methionine at 0.10 M to hem(Cys-His)$_2$ and heme(Cys-His)$_2$ solutions resulted in no significant spectral changes, suggesting that these ligands do not displace one of the dipeptide histidine ligands or that displacement does not produce spectral changes. Addition of pyridine at 0.10 M to hem(Cys-His)$_2$ solutions results in a 5% increase in the intensity of the 528-nm absorption band and a smaller increase in the intensity of the 406-nm band. heme(Cys-His)$_2$ solutions containing 0.10 M pyridine exhibit 550- and 521-nm absorption bands increased about 7% in intensity and the Soret band shifted to 412 nm with 12% less intensity. The magnitude of these spectral changes precluded quantitative study to determine if they reflect pyridine displacement of dipeptide histidine ligands or nonspecific pyridine–porphyrin interactions discussed below.

Heme c and heme(Cys-His)$_2$ in the presence of carbon monoxide show large spectral changes (see Table I). The heme(Cys-His)$_2$ carbon monoxide spectrum resembles that of carbonylated carboxymethylferrocytochrome c,[31] suggesting displacement of one dipeptide histidine ligand, whereas the heme c carbon monoxide spectrum is much like that of iron(II) protoporphyrin with one carbon monoxide ligand and one water ligand.[32] Reversibility of carbon monoxide ligation was demonstrated by restoration of heme(Cys-His)$_2$ and heme c spectra upon removal of carbon monoxide from the anaerobic cell. Equilibrium quotients for CO binding to these iron(II) porphyrins have not yet been determined.

Magnetic Measurements. The low-spin character of hemin c and heme c in solutions containing an excess of the ligands studied above was demonstrated by the NMR magnetic method.[16,18] For 5×10^{-3}–1×10^{-2} M hemin c solutions, the magnetic moments of ligand complexes are as follows: cyanide ion at pH 10.0, 2.5 μ_B; histidine at pH 7.5, 2.3 μ_B; imidazole at pH 9.3, 2.0 μ_B; pyridine at pH 6.1, 2.8 μ_B. Corresponding heme c–ligand complexes as well as the N-acetyl-DL-methionine complex appear to be diamagnetic, with an upper limit of 0.9 μ_B determined by resolution of the NMR spectrometer.

Discussion

In a previous qualitative study of ligand binding to hemin c and heme c, some of the spectra listed in Table I were described.[33] (Mention should also be made of additional absorption bands not listed in Table I for low-spin hemins at ~350 nm, ϵ ~27 000, and low-spin hemes at ~325 nm, ϵ ~32 000). Although our wavelength maxima and molar absorptivity values are in general agreement, inadequacies in the earlier work may have involved using insufficiently high ligand concentrations, using excessively high ligand concentrations (for pyridine in particular), reduction with dithionite ion in the presence of oxygen (most noticeable at the low concentrations used for Soret spectra), and an arbitrary choice of hemin c molecular weight since no analytical data were provided. Our molar absorptivity values, based on the iron content of the hemins,[16] were determined by using eq 6 and/or by extrapolation using solutions with 95–99% ligated iron porphyrin. Additional spectral changes, apparently not associated with ligand–metal binding and more important for aromatic ligands, were noted at somewhat higher ligand concentrations. Similar spectral effects, due to π donor–acceptor or hydrophobic interactions, have been noted for substituted pyridine interaction with metal-free porphyrins.[34,35] Spectral changes observed during our coordination studies are all typical of high-spin to low-spin transitions in iron porphyrins, implying direct ligand coordination.[36] Solution magnetic measurements, although necessarily made under concentration conditions different from those for spectrophotometric measurements, also substantiate spin-state changes upon ligand binding.

Carboxyl and amino groups in L-histidine and methionine potentially may serve as metal ligands, but a variety of evidence supports the imidazole group and sulfur atom for coordination at nearly neutral pH. Acetylamine-blocked histidine and methionine yield spectra equivalent to those for free histidine and imidazole and for free methionine, respectively, at this pH. Equilibrium quotients for these blocked amino acids tend to be higher (due to charge effects) but should be much smaller or zero if amine groups served as ligands. At neutral pH hemin c and heme c solutions 0.5 M in glycine, glutamic acid, or sodium acetate showed only small spectral changes and did not produce low-spin spectra. Apparently two methionine sulfur ligands would provide an insufficiently strong ligand field to force the iron(III) porphyrin to low spin at room temperature. Addition of N-acetyl-DL-methionine at 1.2 M to hemin c solutions did not produce low-spin spectra but did result in a shift of the Soret band to 397 nm. However, visual inspection of N-acetyl-DL-methionine-containing hemin c solutions frozen at 195 K revealed the orange-red color of ligated low-spin hemin c. It should be pointed out that iron(III) protoporphyrin forms low-spin complexes with mercaptans detectable by electron spin resonance at liquid nitrogen temperatures.[37]

Table VII contains enthalpy and entropy values calculated from ligand-binding equilibrium quotients by van't Hoff plots.

Table VII. Thermodynamic Values for Ligand Binding to Iron Porphyrins[a]

Reaction	pH	Q^b	ΔH,[c] kcal/mol	ΔS,[c] eu
Hemin *c* + 2His	6.1	4.7×10^4 M^{-2}	−12.1 ± 0.3	−19.2 ± 0.9
Hemin *c* + 2Im	6.0	1.0×10^6 M^{-2}	−10.8 ± 0.8	−8.7 ± 2.7
Hemin *c* + 2py	6.0	1.1×10^3 M^{-2}	−8.0 ± 0.8	−13.0 ± 2.8
Hemin *c* + CN^-	6.0	2.6×10^5 M^{-1}	−7.5 ± 0.6	−0.4 ± 1.9
Cyanohemin *c* + CN^-	6.0	6.2×10^4 M^{-1}	−7.7 ± 0.5	−3.9 ± 1.6
hem(Cys-His)$_2$ + CN^-	7.0	7.8×10^3 M^{-1}	−8.5 ± 0.7	−10.7 ± 2.2
Heme *c* + 2His	7.0	2.3×10^4 M^{-2}	−16.0 ± 0.6	−33.7 ± 2.1
Heme *c* + 2Im	7.0	1.3×10^5 M^{-2}	−15.1 ± 0.4	−27.3 ± 1.4
Heme *c* + 2py	7.0	4.7×10^5 M^{-2}	−18.8 ± 0.6	−37.1 ± 1.9
Heme *c* + 2(*N*-acetylmethionine)	7.0	6.8×10^2 M^{-2}	−12.6 ± 1.2	−29.3 ± 4.2
Heme *c* + CN^-	6.5	4.6×10^5 M^{-1}	−13.9 ± 0.9	−20.7 ± 2.9
Cyanoheme *c* + CN^-	7.0	7.9×10^3 M^{-1}	−8.6 ± 0.9	−11.0 ± 3.1
heme(Cys-His)$_2$ + CN^-	7.0	8.5×10^4 M^{-1}	−19.4 ± 0.8	−42.5 ± 2.5

[a] $I = 0.10$ with $NaClO_4$; 0.01 M phosphate buffer. [b] Calculated at 25 °C from ΔH and ΔS. [c] Uncertainties represent one standard deviation.

Although direct calorimetric measurements are preferred to the indirect method used here, the higher concentrations required for calorimetry preclude measurements on monomeric iron porphyrins. The data presented here represent the first enthalpy and entropy values reported for ligand binding to monomeric iron porphyrins in aqueous solution, but the limitations of these quantities must be discussed. It is important to note that our equilibrium quotients are valid representations of equilibrium only under conditions specified for a given value. Variations in solution conditions may alter equilibrium quotients slightly (even though ligand protonation and aggregation effects are accounted for) because of complex and incompletely characterized perturbations of solution structure. In general, workers disregard these secondary effects and incorrectly label the equilibrium quotient, Q, as the equilibrium constant, K. As it was not practical to obtain thermodynamic equilibrium constants by extrapolation to zero ionic strength, equilibrium quotients were obtained at constant ionic strength of 0.10. The absence of large differences in equilibrium quotients measured at ionic strengths of 0.025, 0.10, and 0.30 in Table II suggests that the ratio of activity coefficients for Fe(por)L_n and Fe(por) remains nearly constant. Temperature dependence of this activity coefficient ratio is unknown and any dependence will be reflected in enthalpy values. The magnitude of ligand activity coefficients as well as the reliability of published ligand protonation data will also affect enthalpy and entropy values. With that in mind, the quantities listed in Table VII represent estimates of thermodynamic parameters with uncertainties in ΔH perhaps as large as 10% and uncertainties in ΔS on the order of 3–6 eu.

Solution composition was varied to check equilibrium quotients for buffer, iron porphyrin concentration, and pH dependence. Use of phosphate buffer at concentrations lower than 0.01 M and substitution by 0.01 M Pipes (piperazine-*N*,*N*′-bis(2-ethanesulfonic acid)) buffer resulted in no significant changes in equilibrium quotients shown in Tables II and III. Although dimerization equilibria limited the iron porphyrin concentration range over which ligation could be studied, under conditions where hemin *c* is essentially monomeric no significant concentration effects were noted. Increasing amounts of dimeric hemin *c* lower the apparent equilibrium quotient determined by eq 6 as is shown in Table II for L-histidine binding to hemin *c* at 2.8×10^{-5} M (18% dimer) and at pH 7.08 (17% dimer). Equation 8 was used for ligand binding to heme *c* and for solutions up to 3×10^{-5} M (30% dimer) in the case of *N*-acetyl-DL-methionine binding in Table III this analysis appears acceptable, but deviations may occur at higher heme *c* concentrations as suggested by Q_1 values in Table IV.

Hemin *c* ligand binding was studied over the pH range from 5.5 to 6.5 for L-histidine and cyanide ion. Solubility limitations at lower pH and iron(III) hydrolysis with consequent dimerization at higher pH[16] prevented study over a broad pH range. Equilibrium quotients for both histidine and cyanide ion were significantly larger at pH 5.5, perhaps due to decrease in negative charge on the iron porphyrin with protonation of propionic acid side chains. A significant increase in Q_1 for cyanide ion binding to hem(Cys-His)$_2$ at pH 6.5 may be rationalized by favorable protonation of the imidazole group in the displaced dipeptide side chain. Effects of pH for L-histidine, cyanide ion, and *N*-acetylmethionine binding to heme *c* are small and variable and in the case of L-histidine and cyanide ion may reflect uncertainties in the ligand protonation constants.

Due to solvent interactions, experimental enthalpy changes are not simply ligand–metal bond energies. There are contributions from (i) ligand–metal bond formation, (ii) displacement of water (or other) ligands, (iii) changes in solvation of the iron porphyrin upon ligand binding, and (iv) changes in solvation of the bound ligand and any displaced ligands. Since the iron in high-spin iron porphyrins probably lies out of the porphyrin plane,[38] whereas addition of strong-field ligands results in conversion to a low-spin in-plane structure, enthalpy contribution (i) must also reflect possible electron-pairing energies, changes in iron–pyrrole nitrogen bond length, and changes in iron–pyrrole nitrogen orbital overlap. The spin-state change may explain the somewhat more exothermic values in Table VII compared to values of 0.0 to −5.0 kcal/mol typical for single ligand coordination in aqueous solution of first-row transition metal ions in general.[39] Other trends in Table VII also merit discussion. Consistently more exothermic values for heme *c* compared to those for hemin *c* may be accounted for by the energy required to desolvate the more strongly solvated iron(III) species, as well as some degree of π bonding expected for axial ligands bound to iron(II) porphyrins.[5,7,40] Multiple bonding between iron(II) and pyridine serves to explain the large enthalpy and entropy differences observed for hemin *c* and heme *c* binding by this ligand, as well as large differences in equilibrium quotients previously noted for iron(II) and iron(III) protoporphyrin.[5] The highly exothermic cyanide ion binding to heme(Cys-His)$_2$ may be explained by a favorable combination of σ-donor and π-acceptor ligands. Imidazole (of the dipeptide side chain) is a good σ-donor but comparatively poor π-acceptor ligand, whereas the trans cyanide ion is an excellent π acceptor. Favorable combinations of imidazole and the good π-acceptor ligands carbon monoxide and dioxygen are also expected.

Observed entropy changes for ligand binding in aqueous solution also reflect several contributions: (i) decrease due to loss of ligand translational entropy and partial loss of ligand rotational entropy, (ii) increase from displaced solvent or other ligands, (iii) increase from desolvation of reacting ligand, (iv) decrease from solvation of displaced ligand, (v) increase from desolvation of the metalloporphyrin, (vi) decrease from additional rotational entropy loss due to metal–ligand π bonding, and (vii) increase or decrease from molecular weight and

Table VIII. Selected Thermodynamic Values for Ligand Binding to Metalloporphyrins

Metalloporphyrin	*n* ligand[a]	Solvent	Q^b	ΔH, kcal/mol	ΔS, eu	Ref
Iron(II) deuteroporphyrin dimethyl ester	2 py	Benzene	$3.7 \times 10^2\ M^{-2}$	−2.4	+4	7
Iron(II) deuteroporphyrin dimethyl ester	2 py	Benzene	$1.3 \times 10^8\ M^{-2}$	−34.5	−78	12
Iron(II) deuteroporphyrin dimethyl ester	2 py	CCl_4	$4.4 \times 10^2\ M^{-2}$	−14.2	−35	13
Iron(III) tetraphenylporphine	2 Im	Acetone	$7.9 \times 10^4\ M^{-2}$	−19.8	−44	9
Iron(III) tetraphenylporphine	2 Im	Acetone	$6.6 \times 10^5\ M^{-2}$			8[c]
Iron(III) deuteroporphyrin dimethyl ester	2 Im	CH_2Cl_2	$1.2 \times 10^6\ M^{-2}$	−22.0	−46	14
Nickel(II) tetraphenylporphine	1 py	Benzene	$1.4 \times 10^3\ M^{-1}$	−6.3	−7	51
Nickel(II) deuteroporphyrin dimethyl ester	2 pip	$CHCl_3$	$2.1 \times 10^{-2}\ M^{-2}$	−5.5	−26.2	50
Nickel(II) tetraphenylporphine	2 pip	Toluene	$3.5 \times 10^{-1}\ M^{-2}$	−5.6	−21	52
Nickel(II) tetra-*N*-methylpyridylporphine	1 Im, 1 H_2O	Water	$8.4\ M^{-1}$	−10.6	−31.4	43
Iron(III) myoglobin	1 CN^-	Water	$2.3 \times 10^8\ M^{-1}$	−18.6	−24	59
Iron(III) cytochrome *c*	1 CN^-	Water	$1.2 \times 10^6\ M^{-1}$	+1.1	+31.3	59
Iron(III) cytochrome *c*	1 Im	Water	$4.6 \times 10^1\ M^{-1}$	−1.4	+2.9	58

[a] py = pyridine, Im = imidazole, pip = piperidine. [b] At 25 °C. [c] At 30 °C.

structural changes of the iron porphyrin. Term (i) typically accounts for −25 eu per ligand while loss of one water molecule ligand results in +16.7-eu change. Ignoring for the moment terms (iii)–(vii) and assuming hemin *c* and heme *c* contain two axial water ligands (despite the iron lying out of the porphyrin plane), an entropy change of −8 eu per ligand is expected. The other contributions listed above must account for deviations from this expected value in Table VII. A more favorable entropy term for cyanide ion binding to hemin *c* is expected since the neutralization of charge upon ligand binding decreases the solvation number. More positive entropy changes for hemin *c*–ligand binding probably reflect more extensive solvation of the iron(III) compound and thus the enhanced importance of term (v). Also, the well-documented influence of π bonding in iron(II) porphyrin compounds[5,7,40] suggests term (vi) may account for the more negative ΔS values for hemes in Table VII.

Selected values from other ligand-binding studies are listed in Table VIII. Some comparisons with values in Table VII are difficult since previous workers obtained equilibrium quotients differing by more than 5 orders of magnitude for the iron(II) deuteroporphyrin–pyridine system[7,12] and values differing by 1 order of magnitude for the iron(III) tetraphenylporphine–imidazole system.[8,9] Although a wealth of information may be obtained from nonaqueous studies, improper choice of solvent may result in a system far more complex than that for aqueous media. Apparently, solvents should be avoided which are aromatic (due to porphyrin–solvent π donor–acceptor interactions),[14,41,42] which are highly halogenated (due to oxidizing properties),[12] or which cannot be highly purified (e.g., dried).

Differences in solvation and axial binding of solvent molecules are expected to account for thermodynamic differences for ligand binding in aqueous and nonaqueous solvents. Displacement of water ligands and desolvation of the metal center as well as desolvation of the reacting ligand should result in more positive ΔH values in aqueous solution. The entropy term is also expected to be more positive for aqueous solutions primarily due to ligand displacement and solvation terms (ii), (iii), and (v) discussed above. Binding of two axial water ligands to a water-soluble nickel(II) porphyrin resulted in an enthalpy change of −9.4 kcal/mol and an entropy change of −31.1 eu,[43] and binding of a single alcohol or ether ligand to iron(II) deuteroporphyrin dimethyl ester resulted in values of $\Delta H \simeq -5$ kcal/mol and $\Delta S \simeq -16$ eu.[12] When solvation effects are considered, enthalpy values should be at least 10 kcal/mol more negative and entropy values should be at least 32 eu more negative compared to those for heme *c* for iron(II) porphyrin binding in noncoordinating solvents. Thus, for pyridine binding to iron(II) deuteroporphyrin dimethyl ester in benzene, we expect $\Delta H < -29$ kcal/mol and $\Delta S < -69$ eu. Values of $\Delta H = -34.5$ kcal/mol and $\Delta S = -78$ eu in ref 12 are satisfying, whereas values in ref 7 and 13 (Table VIII) seem unreasonable. Solvation is expected to be more important for iron(III) porphyrins, and comparisons are somewhat more complicated by the coordinated counterion in nonaqueous media. However, enthalpy and entropy differences on the order of 10 kcal/mol and 36 eu are observed when imidazole binding to aqueous hemin *c* is compared to binding by iron(III) tetraphenylporphine or iron(III) deuteroporphyrin in nonaqueous media (see Table VIII).

Surprisingly, only one imidazole ligand binds to an iron(III) ethylenediamine protoporphyrin derivative and to iron(III) deuteroporphyrin-2,4-disulfonic acid in aqueous solution.[44,45] Perhaps the ligand field of these porphyrins is modified such that one imidazole ligand is sufficient to yield low-spin iron(III). Charge effects must also be important for such porphyrins with "unnatural", highly charged side chains. A possibility not considered by the authors of ref 44 involves coordination of an ethylenediamine side chain as well as imidazole. Two imidazole ligands bind to iron(III) protoporphyrin in aqueous detergent media.[46]

Binding of a single strong-field cyanide ligand is sufficient to produce low-spin hemin *c* and heme *c*, although no mention was made of stepwise binding in the earlier qualitative study.[33] Only the overall addition of two cyanide ions has been observed in aqueous detergent solutions.[6,47] Effects attributable to the detergent must eliminate the single cyanide ion stoichiometry, as stepwise coordination of cyanide ion to iron(III) protoporphyrin has been reported for basic aqueous solution and dimethyl sulfoxide solvent.[48]

Thermodynamic studies of ligand binding to nickel(II),[43,49-52] copper(II),[49] zinc(II),[51,53] magnesium(II),[53] vanadium(IV),[52] cadmium(II),[53] and mercury(II)[53] metalloporphyrins have also been carried out. Nickel(II) porphyrin equilibria with pyridines and piperidine have received the most attention and involve adding either one or two ligands to the diamagnetic square-planar compound to yield paramagnetic square-pyramidal or octahedral complexes, respectively. Nickel(II) porphyrins have been employed to show that the enthalpy of ligand binding is directly related to porphyrin basicity,[50] and a Hammett relationship was found for phenyl-substituted nickel(II) tetraphenylporphine derivatives.[52] Typical thermodynamic parameters for Ni(II) porphyrins in Table VIII show that the enthalpies for ligand binding are considerably less favorable than corresponding values for iron(II) porphyrins. Unfavorable enthalpies are partially compensated by more favorable entropies.[50] Differences for imidazole binding to nickel(II) tetra-*N*-methylpyridylporphine and to heme *c* (both in water) are even more striking when the energy to displace axial water ligands ($\sim$10 kcal/mol) in heme *c* is taken into account (the reacting nickel species is apparently square planar). Less favorable ligand binding to nickel(II) porphyrins is expected, since a stronger porphyrin–metal bond is associated with a weaker axial bond,[50] and nickel(II) porphyrins are considerably more stable with respect

to metal displacement than iron(II) porphyrins.[54]

Thermodynamic parameters for ligand binding to two hemoproteins are listed in Table VIII. More negative enthalpy and entropy values for myoglobin compared to those for hemin *c* cyanide ion binding may be explained in part by the diminished solvation of the iron porphyrin in the hydrophobic interior of the hemoprotein. Comparison of cyanide ion and imidazole binding to hemin *c* and ferricytochrome *c* suggests that conformation changes must dominate the thermodynamics of ligand binding in this enzyme. Estimates of $\Delta H = -18.0$ kcal/mol and $\Delta S = -48.0$ eu for closing of the ferricytochrome *c* crevice support this supposition.[55,56] Comparison of ligand binding to iron porphyrins with similar measurements on hemoproteins suggests that details of ligand interactions may be obscured by changes in protein conformation. Attempts to fit our iron porphyrin data to enthalpy–entropy compensation plots for hemoglobin[57] and cytochrome *c*[58] were unsuccessful. Although incompletely understood, the compensation phenomenon appears to involve rearrangement of solvent on the surface of the protein, and the divergence of the iron prophyrin data from compensation behavior supports involvement of the polypeptide chain. The results presented here should be of value in other thermodynamic hemoprotein studies and hopefully will replace the often quoted but questionable values in ref 7. Knowledge of ligand-binding constants for a water-soluble iron porphyrin will also allow redox and site of interaction experiments for ligated iron porphyrins and hemoproteins.

Acknowledgment. This work was supported by the Robert A. Welch Foundation, Houston, Tex. (Grant No. F-041).

Registry No. Hemin *c*, 26219-53-4; dihistidylhemin *c* analog, 59671-74-8; bis(imidazole)hemin *c* analog, 59727-95-6; bis(pyridine)hemin *c* analog, 59671-75-9; cyanohemin *c* analog, 59671-76-0; dicyanohemin *c* analog, 59727-94-5; hem(Cys-His)$_2$, 59727-58-1; hem(Cys-His)$_2$(CN), 59686-34-9; heme *c*, 26598-29-8; dihistidylheme *c*, 59727-59-2; bis(imidazole)heme *c*, 59671-77-1; bis(pyridine)heme *c*, 59727-60-5; bis(*N*-acetylmethionyl)heme *c*, 59671-78-2; cyanoheme *c*, 59727-61-6; dicyanoheme *c*, 59671-79-3; carbonylheme *c*, 59671-80-6; heme(Cys-His)$_2$, 59671-73-7; heme(Cys-His)$_2$(CN), 59686-36-1; heme(Cys-His)$_2$(CO), 59686-35-0.

References and Notes

(1) R. Hill, *Proc. R. Soc. London, Ser. B*, **105**, 112 (1929).
(2) J. Shack and W. M. Clark, *J. Biol. Chem.*, **171**, 143 (1947).
(3) R. W. Cowgill and W. M. Clark, *J. Biol. Chem.*, **198**, 33 (1952).
(4) H. S. Olcott and A. Lukton, *Arch. Biochem. Biophys.*, **93**, 666 (1961).
(5) J. E. Falk, "Porphyrins and Metalloporphyrins", Elsevier, London, 1964, pp 45–52.
(6) J. Simplicio, *Biochemistry*, **11**, 2525 (1972).
(7) S. J. Cole, G. C. Curthoys, and E. A. Magnusson, *J. Am. Chem. Soc.*, **92**, 2991 (1970).
(8) C. L. Coyle, P. A. Rafson, and E. H. Abbott, *Inorg. Chem.*, **12**, 2007 (1973).
(9) J. M. Duclos, *Bioinorg. Chem.*, **2**, 263 (1973).
(10) M. Momenteau, *Biochim. Biophys. Acta*, **304**, 814 (1973).
(11) D. Brault and M. Rougee, *Biochem. Biophys. Res. Commun.*, **57**, 654 (1974).
(12) D. Brault and M. Rougee, *Biochemistry*, **13**, 4591 (1974).
(13) S. J. Cole, G. C. Curthoys, and E. A. Magnusson, *J. Am. Chem. Soc.*, **93**, 2153 (1971).
(14) E. H. Abbott and P. A. Rafson, *J. Am. Chem. Soc.*, **96**, 7378 (1974).
(15) The convention is followed here in that hemin refers to the iron(III) porphyrin and heme refers to the iron(II) porphyrin.
(16) H. Goff and L. O. Morgan, *Inorg. Chem.*, preceding paper in this issue.
(17) A. I. Vogel, "Quantitative Inorganic Analysis", 3d ed, Longmans, Green and Co., London, 1961, pp 271–272.
(18) D. F. Evans, *J. Chem. Soc.*, 2003 (1959).
(19) R. W. Ramette, *J. Chem. Educ.*, **44**, 647 (1967).
(20) (a) N. J. Rose and R. S. Drago, *J. Am. Chem. Soc.*, **81**, 6138 (1959); (b) R. M. Guidry and R. S. Drago, *ibid.*, **95**, 6645 (1973).
(21) J. S. Coleman, L. P. Varga, and S. H. Mastin, *Inorg. Chem.*, **9**, 1015 (1970).
(22) A. C. Andrews and J. K. Romary, *J. Chem. Soc.*, 405 (1964).
(23) S. P. Datta and A. K. Grzybowski, *J. Chem. Soc. A*, 1059 (1966).
(24) L. Sacconi, P. Paoletti, and M. Ciampolini, *J. Am. Chem. Soc.*, **82**, 3831 (1960).
(25) R. B. Martin and J. T. Edsall, *J. Am. Chem. Soc.*, **82**, 1107 (1960).
(26) D. E. Sands, *J. Chem. Educ.*, **51**, 473 (1974).
(27) R. M. Izatt, J. J. Christensen, R. T. Pack, and R. Bench, *Inorg. Chem.*, **1**, 828 (1962).
(28) F. J. C. Rossotti and H. Rossotti, "The Determination of Stability Constants", McGraw-Hill, New York, N.Y., 1961, p 277.
(29) K. P. Ang, *J. Phys. Chem.*, **62**, 1109 (1958).
(30) R. H. Moore and R. K. Zeigler, Report LA-2367, Los Alamos Scientific Laboratory, Los Alamos, N.M., Oct 1959.
(31) M. T. Wilson, M. Brunori, G. C. Rotilio, and E. Antonini, *J. Biol. Chem.*, **248**, 8162 (1973).
(32) J. Keilin, *Biochem. J.*, **45**, 440 (1949).
(33) N. Nanzyo and S. Sano, *J. Biol. Chem.*, **243**, 3431 (1968).
(34) P. Mohr and W. Scheler, *Eur. J. Biochem.*, **8**, 444 (1969).
(35) M. Tohjo, Y. Nakamura, K. Kurihara, T. Samejima, Y. Hachimori, and K. Shibata, *Arch. Biochem. Biophys.*, **99**, 222 (1962).
(36) One of our referees mentioned the possibility of pyridine reduction of the iron(III) to the iron(II) porphyrin, because such reductions have been observed in nonaqueous systems. We saw no spectral evidence for heme *c* species during the hemin *c*–pyridine measurements even under anaerobic conditions, and the magnetic moment of the hemin *c*–pyridine complex supports the iron(III) oxidation state. In addition, a question was raised about the use of Soret spectra to determine stoichiometry. Reference was made to nickel(II) porphyrin systems which show complex square-planar, square-pyramidal, and octahedral equilibria.[43,49,50] Although we cannot rule out single-ligand addition to hemin *c* or heme *c* with no accompanying spectral changes, the equilibria assigned here appear to be straightforward. Adequate fits to eq 6, eq 8, CVM plots, and Rose–Drago criteria of both Soret-wavelength and visible-wavelength data seem to confirm our interpretations.
(37) A. Roder and E. Bayer, *Eur. J. Biochem.*, **11**, 89 (1969).
(38) J. L. Hoard, M. J. Harmor, T. A. Harmor, and W. S. Caughey, *J. Am. Chem. Soc.*, **87**, 2312 (1965).
(39) F. J. C. Rossotti, "Modern Coordination Chemistry", J. Lewis and R. C. Wilkins, Ed., Interscience, New York, N.Y., 1960, pp 1–77.
(40) W. S. Caughey, E. Eberspaecher, W. H. Fuchsman, and S. McCoy, *Ann. N.Y. Acad. Sci.*, **153**, 722 (1969).
(41) D. Mauzerall, *Biochemistry*, **4**, 1801 (1965).
(42) G. N. La Mar, J. D. Satterlee, and R. V. Snyder, *J. Am. Chem. Soc.*, **96**, 7137 (1974).
(43) R. F. Pasternack, E. G. Spiro, and M. Teach, *J. Inorg. Nucl. Chem.*, **36**, 599 (1974).
(44) G. B. Kolski and R. A. Plane, *J. Am. Chem. Soc.*, **94**, 3740 (1972).
(45) G. B. Kolski and R. A. Plane, *Ann. N.Y. Acad. Sci.*, **206**, 604 (1973).
(46) J. Simplicio, K. Schwenzer, and F. Maenpa, *J. Am. Chem. Soc.*, **97**, 7319 (1975).
(47) J. Simplicio and K. Schwenzer, *Biochemistry*, **12**, 1923 (1973).
(48) J. T. Wang, H. J. C. Yeh, and D. F. Johnson, *J. Am. Chem. Soc.*, **97**, 1968 (1975).
(49) E. W. Baker, M. S. Brookhart, and A. H. Corwin, *J. Am. Chem. Soc.*, **86**, 4587 (1964).
(50) B. D. McLees and W. S. Caughey, *Biochemistry*, **7**, 642 (1968).
(51) S. J. Cole, G. C. Curthoys, E. A. Magnusson, and J. N. Phillips, *Inorg. Chem.*, **11**, 1024 (1972).
(52) F. A. Walker, E. Hui, and J. M. Walker, *J. Am. Chem. Soc.*, **97**, 2390 (1975).
(53) J. R. Miller and G. D. Dorough, *J. Am. Chem. Soc.*, **74**, 3977 (1952).
(54) P. Hambright, *Coord. Chem. Rev.*, **6**, 247 (1971).
(55) E. Margoliash and A. Schejter, *Adv. Protein Chem.*, **21**, 113 (1966).
(56) T. A. Moore and C. Greenwood, *Biochem. J.*, **149**, 169 (1975).
(57) R. Lumry, "Probes of Structure and Function of Macromolecules and Membranes", Vol. II, B. Chance, Y. Yonetani, and A. S. Mildvan, Ed., Academic Press, New York, N.Y., 1971, pp 353–366.
(58) M. Ikeda-Saito and T. Iizuka, *Biochim. Biophys. Acta*, **393**, 335 (1975).
(59) P. George and G. I. H. Hanania, *Nature (London)*, **175**, 1034 (1955).